SAND2021-14177PE

Ultra-Low Frequency Atomic E-field Sensing

Yuan-Yu Jau

Organization of AO Sensing & EC Engineering

Sandia National Laboratories

UNM OSE Seminar 11/11/2021

Sandia National Laboratories is a multimission laboratory managed and operated by National Technology & Engineering Solutions of Sandia, LLC, a wholly owned subsidiary of Honeywell International Inc., for the U.S. Department of Energy's National Nuclear Security Administration under contract DE-NA0003525.

Why atomic sensors?

1. Atomic sensors use the internal energy states with photon-atom interactions that are sensitive to the specific physics quantities of interest, **such as time, magnetic field, velocity, rotations, etc.**
2. The sensing approach are usually accomplished via measuring the frequency shifts, which have coefficients only determined by the fundamental constants. Therefore, **they are precise and accurate!**

Atomic Clock

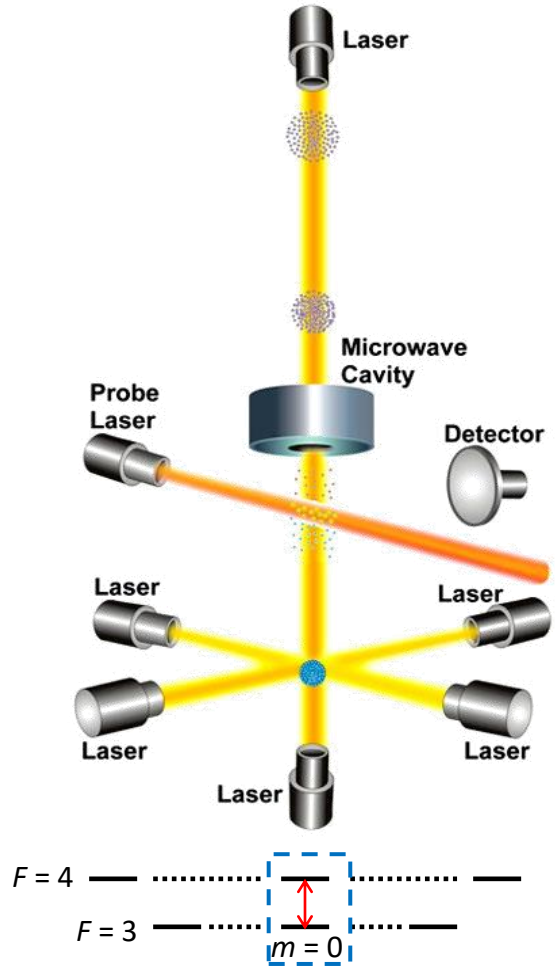

^{133}Cs fountain clock uses hyperfine 0-0 clock transition

Atom Interferometer

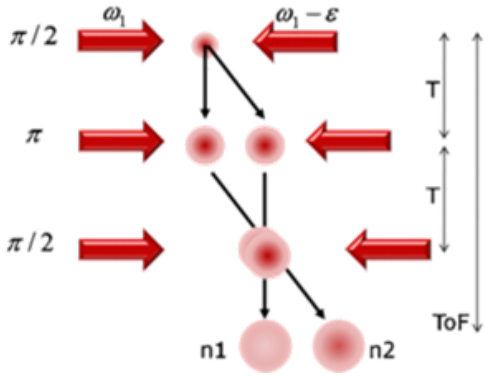

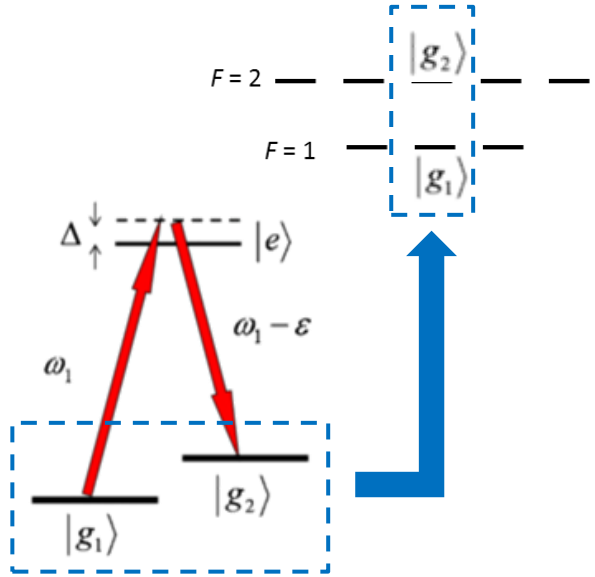

Example: ^{87}Rb atom interferometer utilizes hyperfine clock states as well.

Atomic Magnetometer

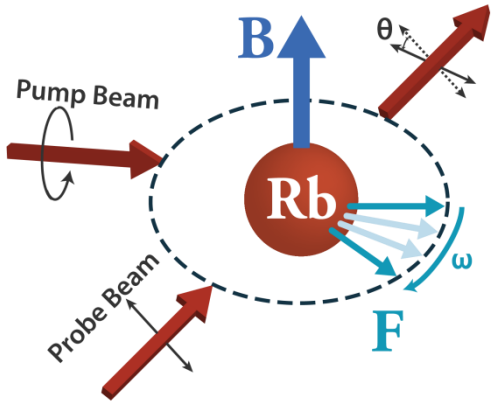

Atomic magnetometer takes advantage of magnetic-sensitive hyperfine transitions.

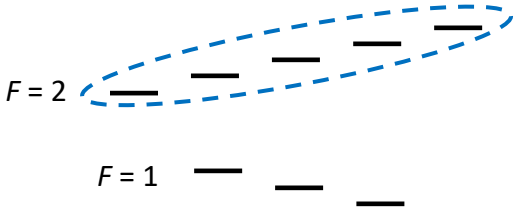

Hyperfine sublevels of Rb-87 in a magnetic field.

Atomic metrology demonstrates state-of-the-art performance

- **Atomic clocks:** Using stable atomic resonances (microwave or optical) for time keeping. Best reported accuracy and precision $\leq 10^{-18}$ (optical clock)
- **Atomic magnetometers:** Using B-field sensitive atomic resonances to measure magnetic field strength. Best reported sensitivity $< 10^{-15}$ tesla/Hz$^{1/2}$ (SERF magnetometer)
- **Atomic accelerometers:** Using atom interferometry technique to measure acceleration. Best reported sensitivity $\sim 10^{-9}$ g/Hz$^{1/2}$
- **Atomic gyroscopes:** Using atom interferometry technique or nuclear spin to measure rotation. Best reported ARW $< 10^{-4}$ deg/h$^{1/2}$

These are the best performing results in the existing sensing technologies.

How about atomic electrometry (atomic E-field sensing)?

- Atoms do have electric-field (E-field) sensitive energy states, the Rydberg states that can be used for E-field sensing.
- In the past decade, Rydberg atomic electrometers have been broadly demonstrated but mainly aiming at traceable standards for RF and microwave frequency range.
- The low-frequency atomic electrometry was rarely investigated before until the recent work at Sandia.

Why ultra-low frequency atomic E-field sensing?

- Although Rydberg atomic electrometers have been widely demonstrated at RF frequencies, **their E-field sensitivity has not surpass the existing electronic RF receivers**.
- **Usually atomic sensors deliver better performance at low detection frequencies compared to the electronic technologies.** For example, atomic magnetometers are only better than a pick-up coil when the detection frequency is below 1 MHz.
- Atomic electrometry shares the same concept. **Sandia has demonstrated that ultra-low frequency (< 3 kHz) atomic electrometry outperform the existing electronic E-field sensors.**

Performance of electronic E-field sensors and RF receivers

Red shade: Calculated low-frequency E-field noise floor using 1-cm antenna with the best commercial transistors or op amps.

Blue shade: Calculated RF E-field noise floor using 1-cm antenna with the best commercial transistors or op amps.

Red circles: Demonstrated E-field sensitivity using 1-cm dipole antenna.

Blue star: Commercial cell phones

Green star: Small GPS receivers

Brown line: Blackbody noise at 300 K

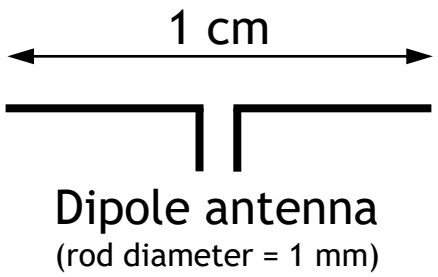

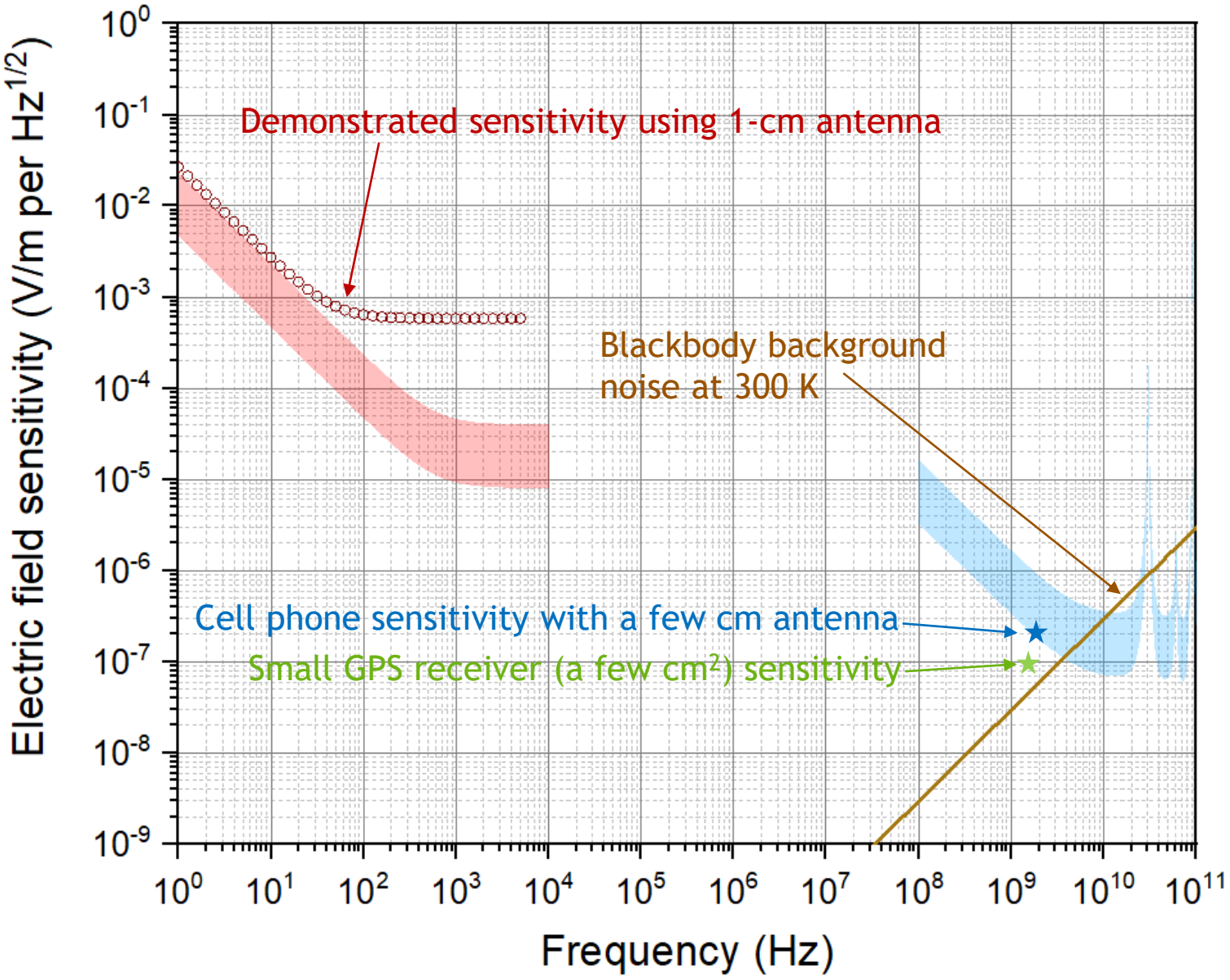

Performance of demonstrated atomic electrometers

Orange shade: Sandia demonstrated in-vapor sensitivity of low-frequency vapor-cell based atomic electrometer with 1.4 cm laser beam path lenght.

Purple points: Other demonstrated vapor-cell based RF atomic electrometers with 5 cm laser beam path length.

Grey shade: Theoretically achievable sensitivity of a Rydberg electrometer.

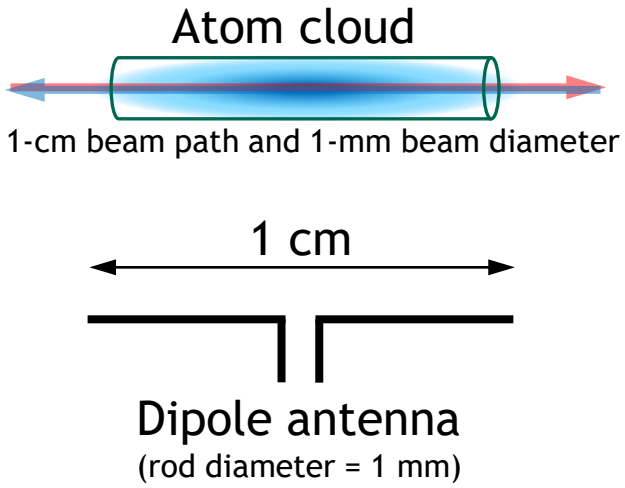

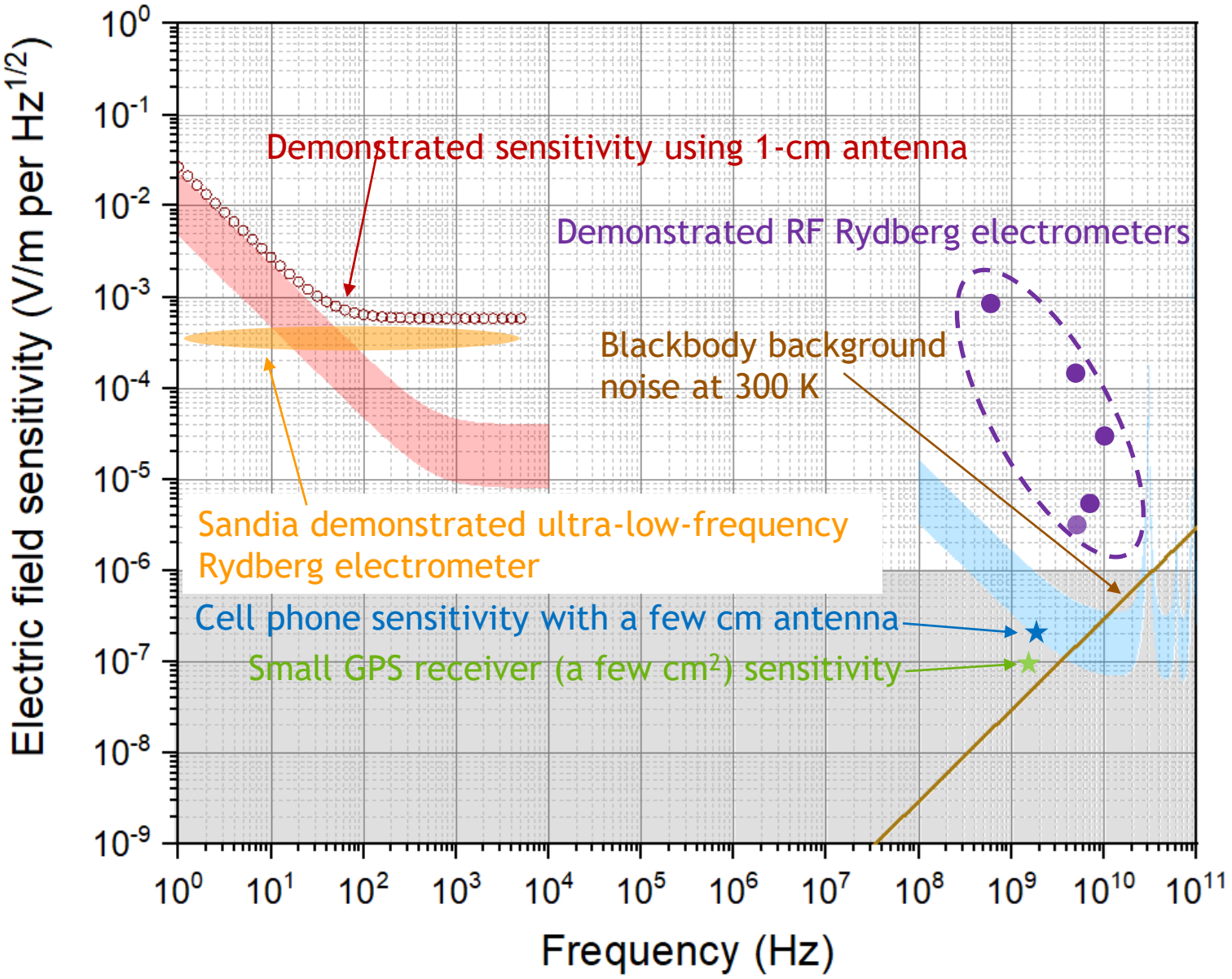

Low-frequency atomic E-field sensing can be much better

From the comparison chart in the previous slide, we see why ultra-low frequency atomic E-field sensing is highly motivated.

None of the demonstrated RF atomic electrometry shows better sensitivity than electronic detection technologies. Further improvement is getting more challenging, since it is approaching to a theoretical limit.

We have demonstrated better performance in low-frequency E-field sensing than the existing electronic technology, and we can do better in the future.

Picture of atomic Rydberg states

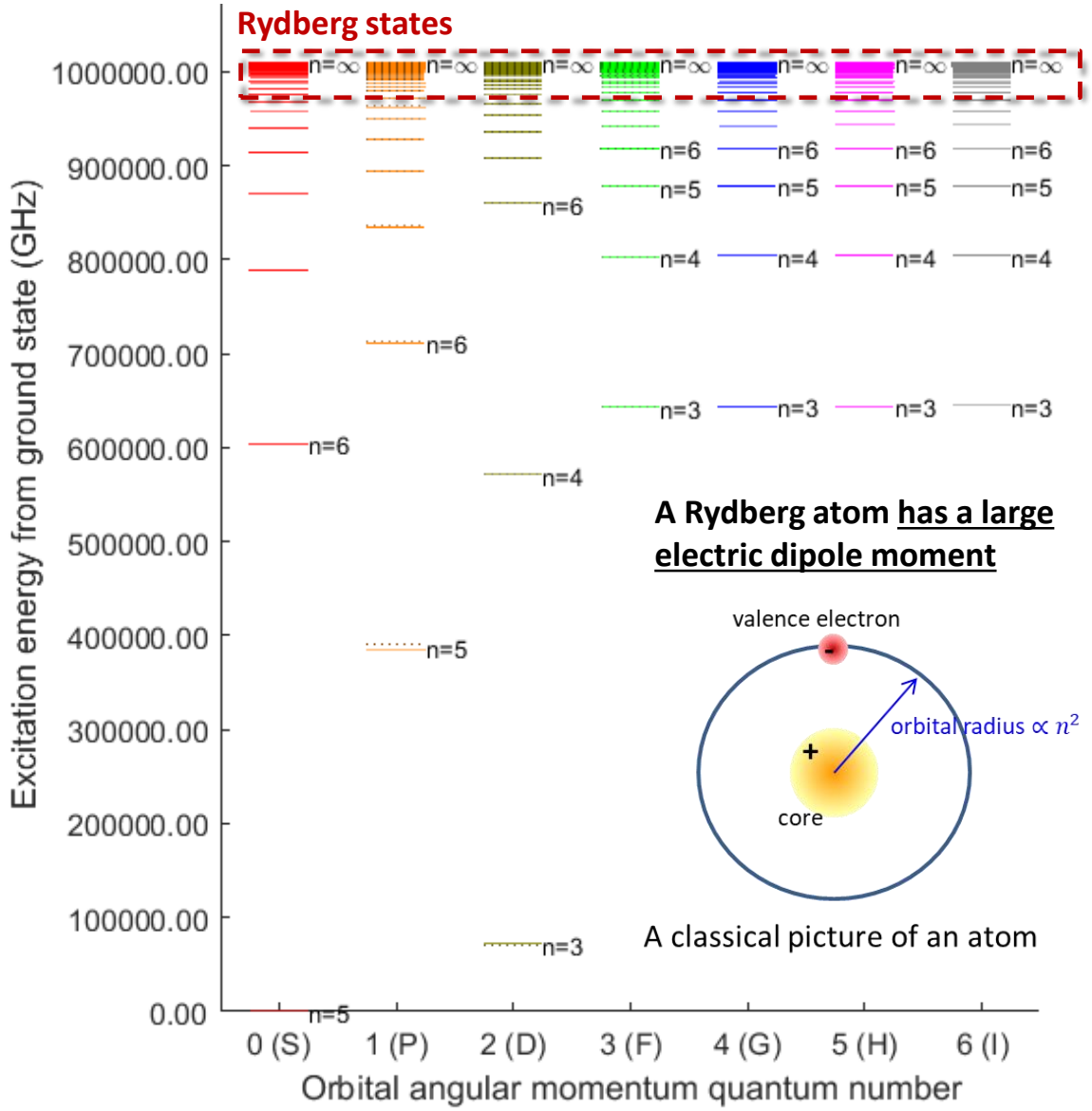

A Rydberg atom <u>has a large electric dipole moment</u>

A classical picture of an atom

Radial wavefunctions of Rb Rydberg states with principal quantum number n = 100 and different orbitals (*S, P, D*)

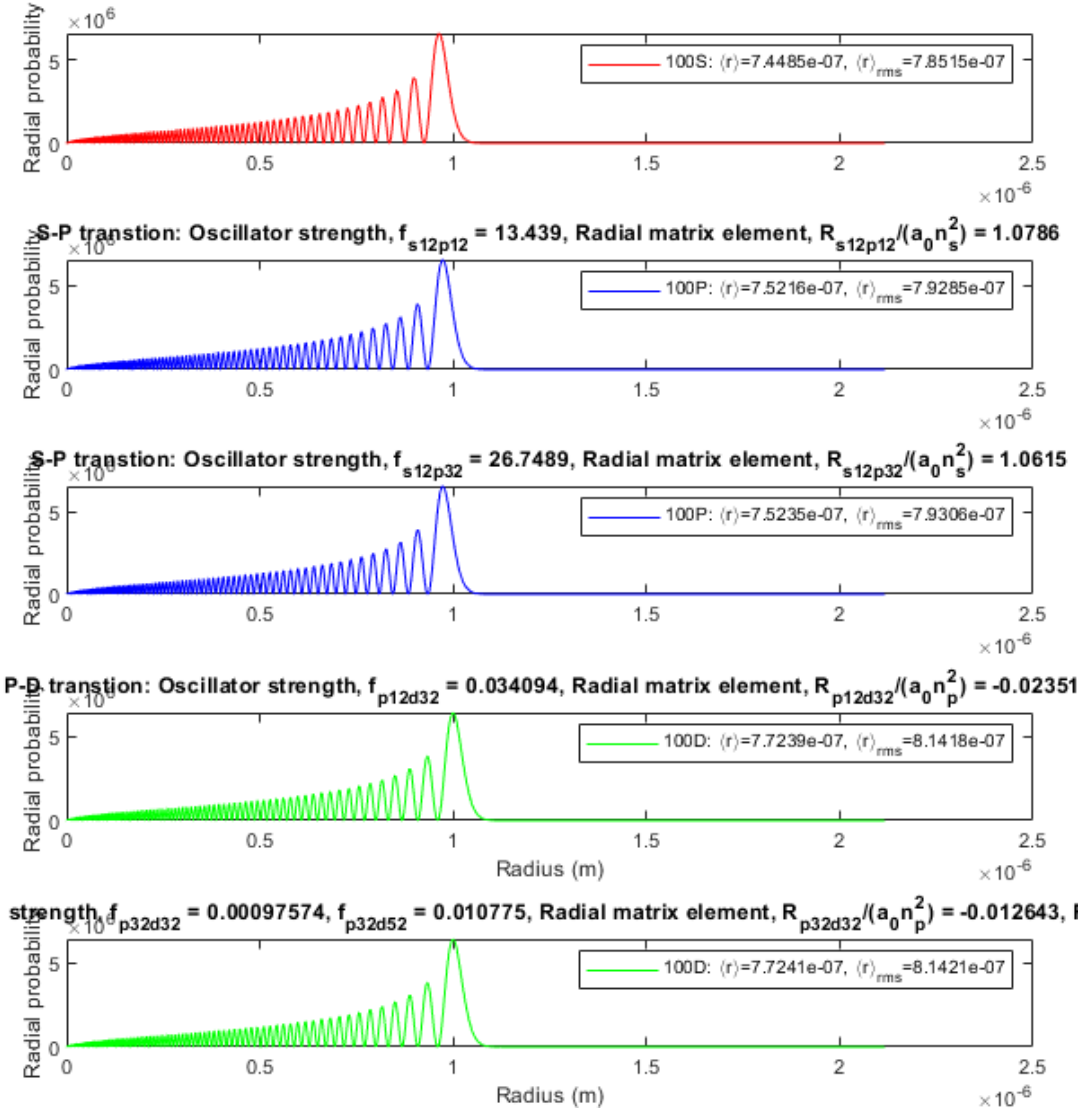

Calculation of Rydberg state energy

For an ideal hydrogen atom with only Coulomb interaction between the electron and the proton and with infinite core mass, we find

$$E_n = -\frac{R_\infty}{n^2}, \text{ where } R_\infty = \frac{m_e e^4}{8\varepsilon_0^2 h^2} \text{ (SI unit Rydberg constant)} \sim 13.6 \text{ eV}$$

For a real atom with A > 1, because of the existing core electrons, we introduce a 1st-order correction to the Rydberg formula:

$$E_n = -\frac{R_\infty}{(n-\delta)^2},$$

where δ is called the quantum defect. With higher-order corrections, we find a more precisely described quantum-defect formula to be:

$$E_n = -\frac{R_\infty}{\left(n - \delta - \frac{\alpha}{(n-\delta)^2} - \frac{\beta}{(n-\delta)^4} - \frac{\gamma}{(n-\delta)^6} - \cdots\right)^2}$$

Here, the parameters $\delta, \alpha, \beta, \gamma, \cdots$ are experimentally determined.

Probing a Rydberg state

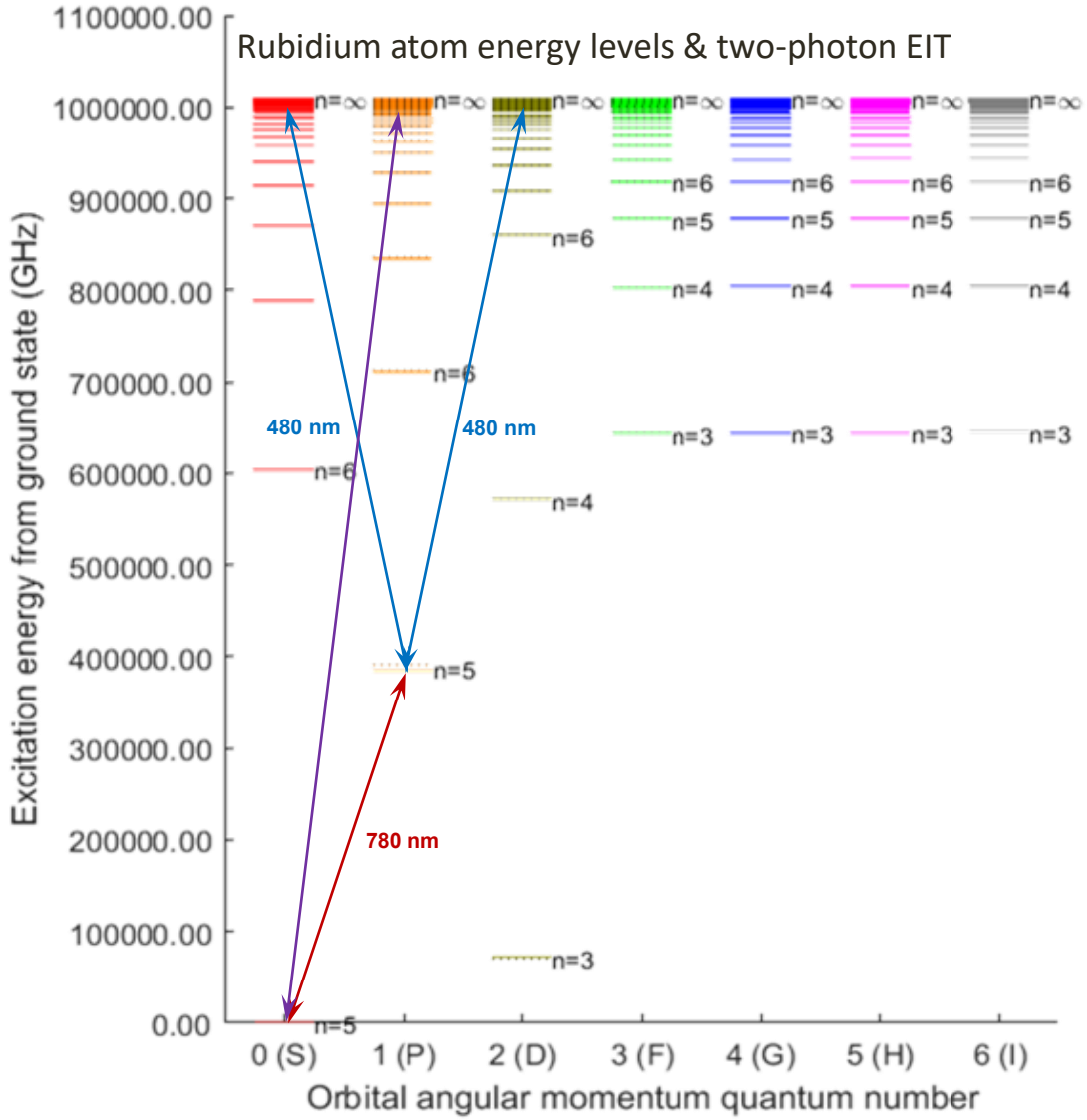

Atomic Rydberg states can be probed via single-photon excitation with a UV laser source. But it is more technically challenging. Generally, a two-photon stimulated Raman transition (electromagnetically induced transparency, EIT) is a more preferred method.

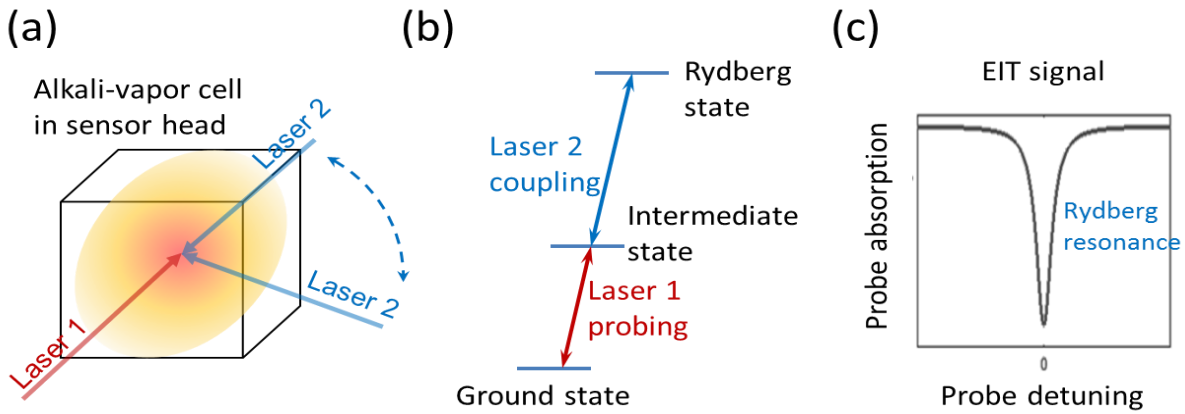

The EIT approach allows the use of more mature laser technology at visible and near-IR wavelengths, and it is perfect for accessing atoms inside an alkali-vapor cell. The Rydberg resonance reveals when both laser 1 and laser 2 are resonant with the associated energy states. Under this circumstance, a superposition state of the ground state and the Rydberg state is generated, and photons are virtually scattered between two laser fields.

Review of RF Rydberg electrometry

On the right: we find a energy level structure of *n* near 100 for *S*, *P*, and *D* orbitals and using $100S_{1/2}$ as a frequency reference.

By coupling a microwave (MW) field between the two adjacent Rydberg states, we see an energy-level splitting.

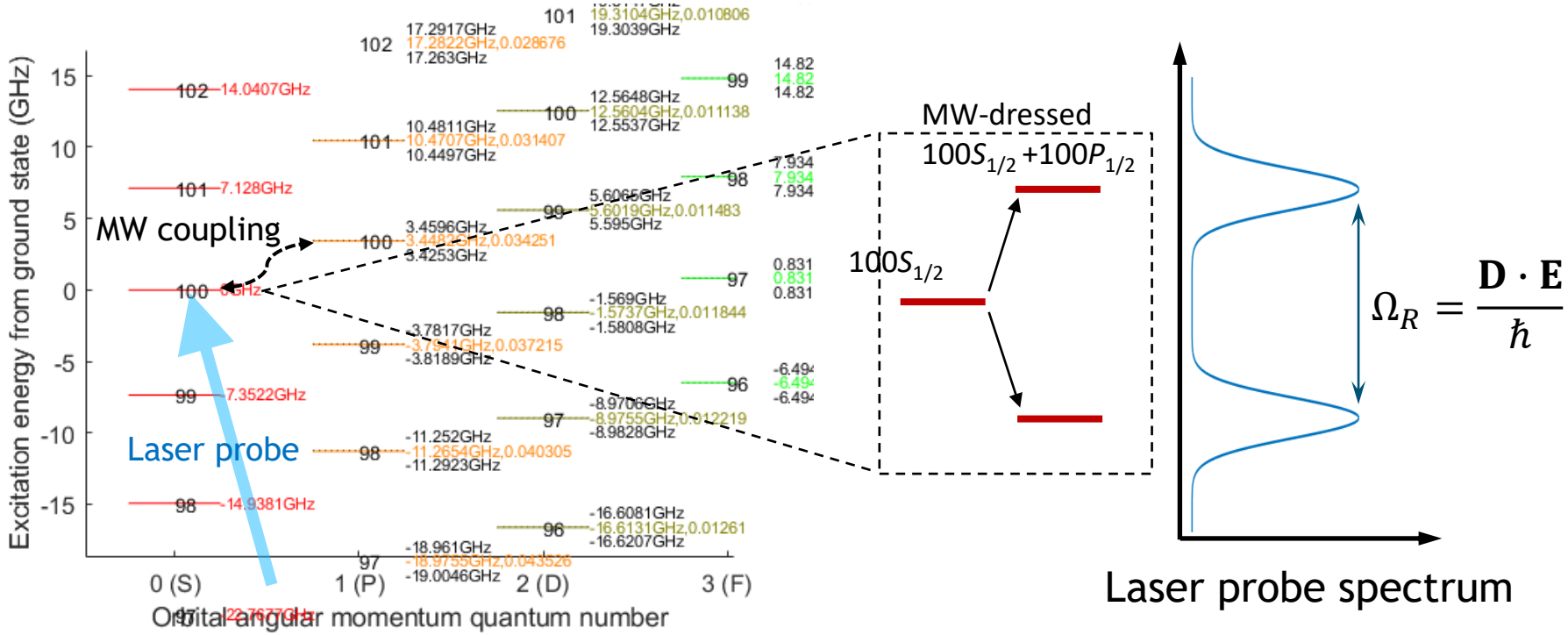

The energy-level splitting is proportional to the Rabi frequency Ω_R, which is proportional to electric-field strength $|\mathbf{E}|$ with a coefficient determined by $\hbar$ and an electric dipole moment $\mathbf{D}$ that can be calculated using fundamental constants. To be noted, $|\mathbf{D}| = \langle er \rangle \approx en^2 a_0$, where r is a classical radius, e is the electron charge, and a_0 is Bohr radius. We believe atoms are the same every where in the universe. **Hence, Rydberg electrometers can be used as E-field standards.**

The downside of this approach is that the measured RF field has to be resonant with a specific microwave transition between Rydberg states. **More recently, heterodyne methods were invented by multiple research group (including Sandia). The detection frequency is no longer limited to discrete transition frequencies.**

Quasi-DC and low-frequency Rydberg electrometry

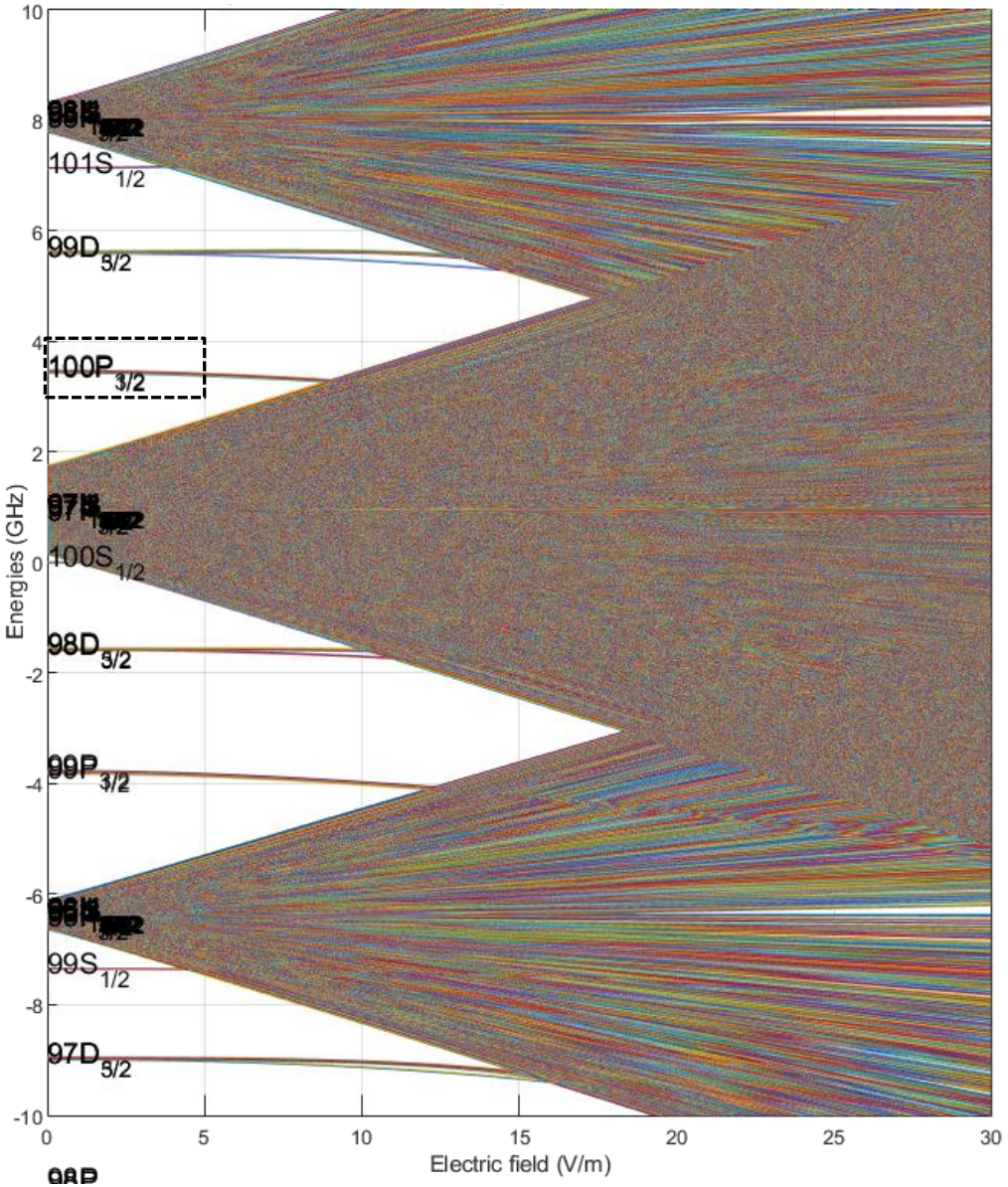

When applying DC electric field or low-frequency electric field to a rubidium (Rb) atom, the Rydberg energy levels near *n* = 100 as functions of E-field amplitude is shown on the left.

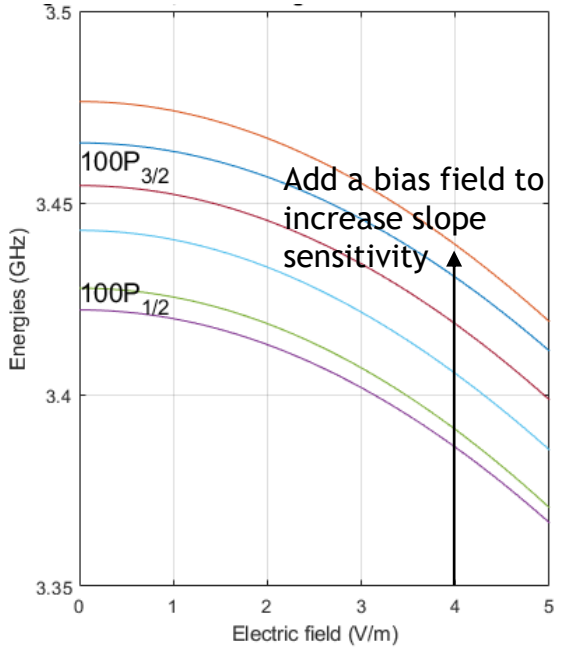

By zooming in, we find the level splittings due to magnetic field and E-field dependent quadratic frequency shift υ.

$$\upsilon = \frac{1}{2\pi}\Sigma_i\left(\frac{\mathbf{D}_i\cdot\mathbf{E}}{4\Delta_i\hbar}\right)^2,$$

where $\mathbf{D}_i$ is the dipole moment of a pair of Rydberg states, Δ_i is the splitting between a pair of Rydberg state, and i is the index of pairs. **This quadratic dependence, however, makes it very insensitive to small E-field signals.**

In order to make the change in the shift frequency $\delta\upsilon$ sensitive to the change of electric field δE, we can introduce a bias E-field E_b, therefore, we find $\delta\upsilon \propto 2E_b\delta E$. The sensitivity is then enhanced by a factor of $2E_b/\delta E$. **This is actually an heterodyne scheme at the DC range. The same method has been recently used in RF Rydberg electrometry to improve the sensitivity and detection frequency range.**

Experimental schematic

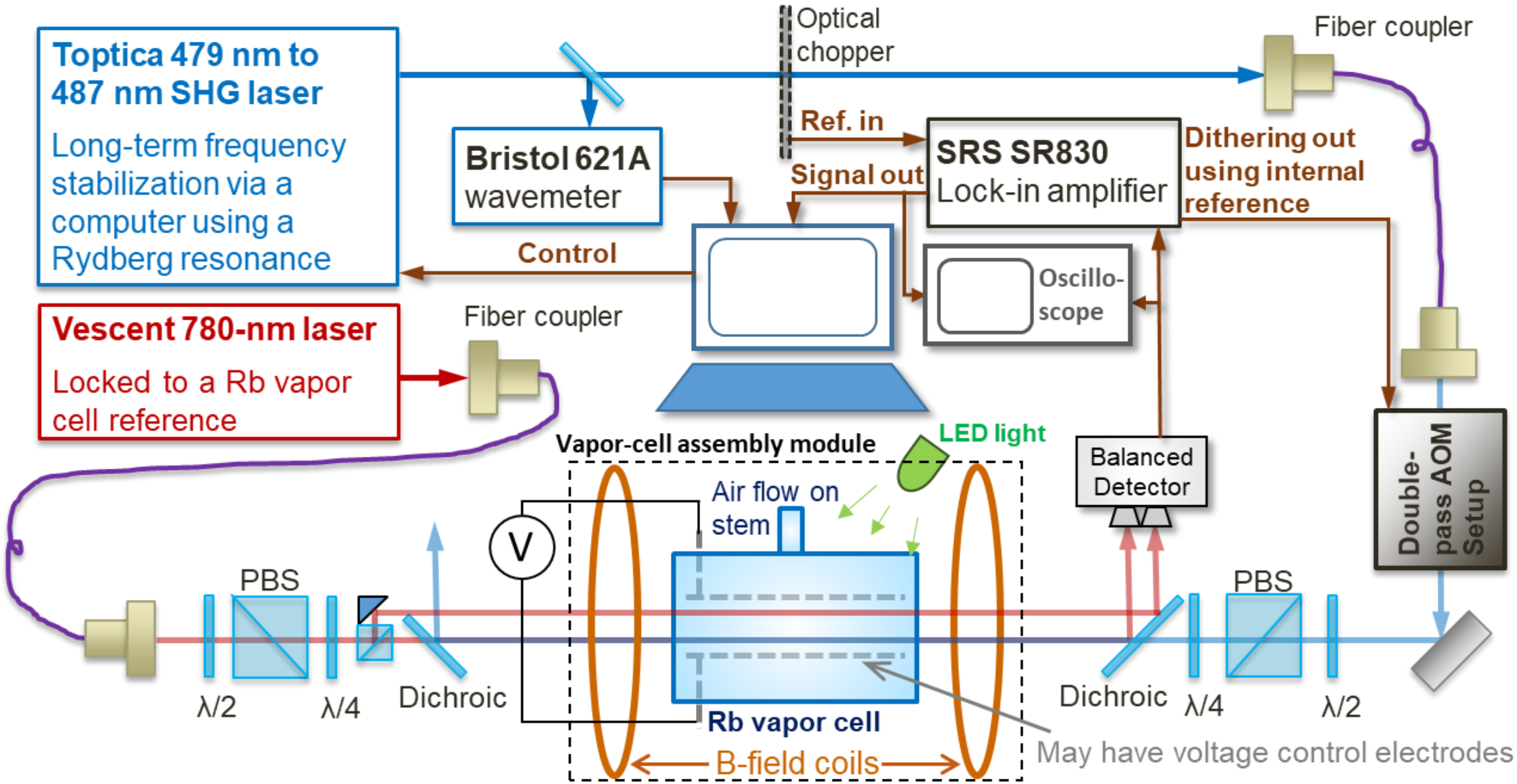

Pictures of experimental apparatus

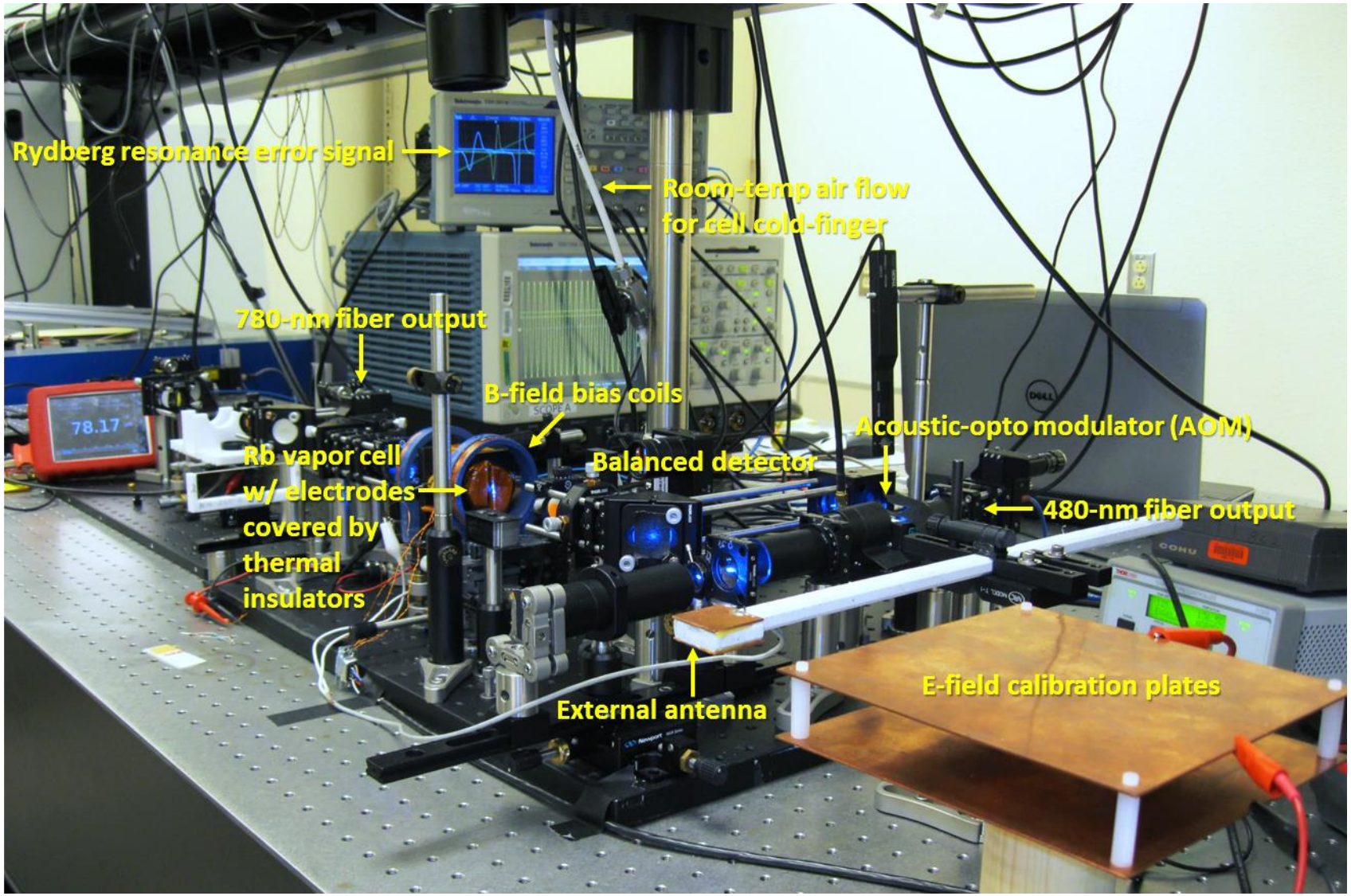

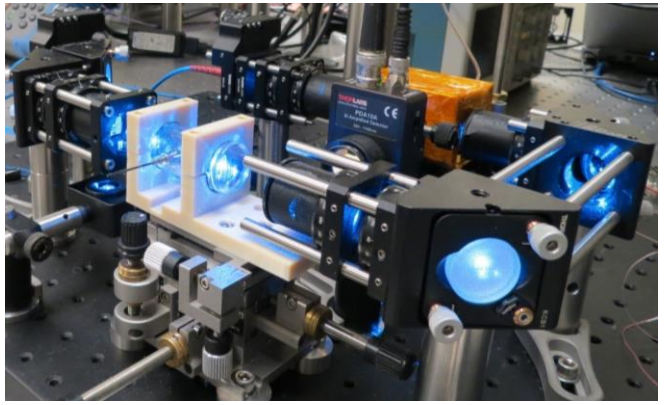

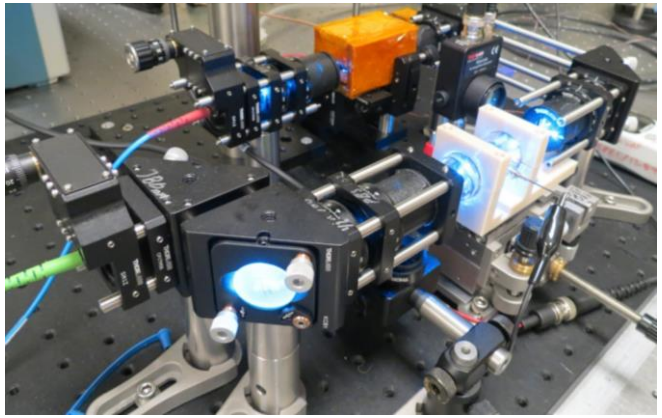

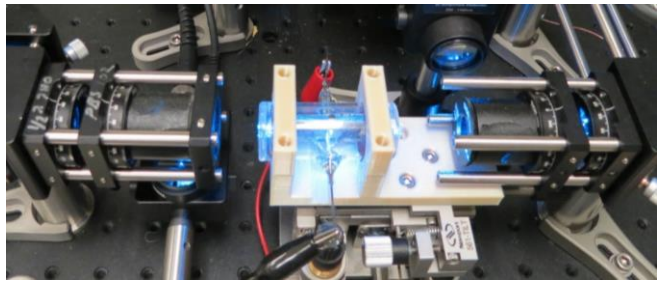

Measurement and modeling of E-field dependent frequency shifts

Using a vapor cell with internal parallel electrodes, we are able to produce well-controlled electric field to the Rb atoms inside the vapor cell to measure the E-field dependent frequency shifts for different Rydberg states. The two figures below show very good match between the modeling result and the experimental data regarding the frequency-shift curves and the relative signal strength.

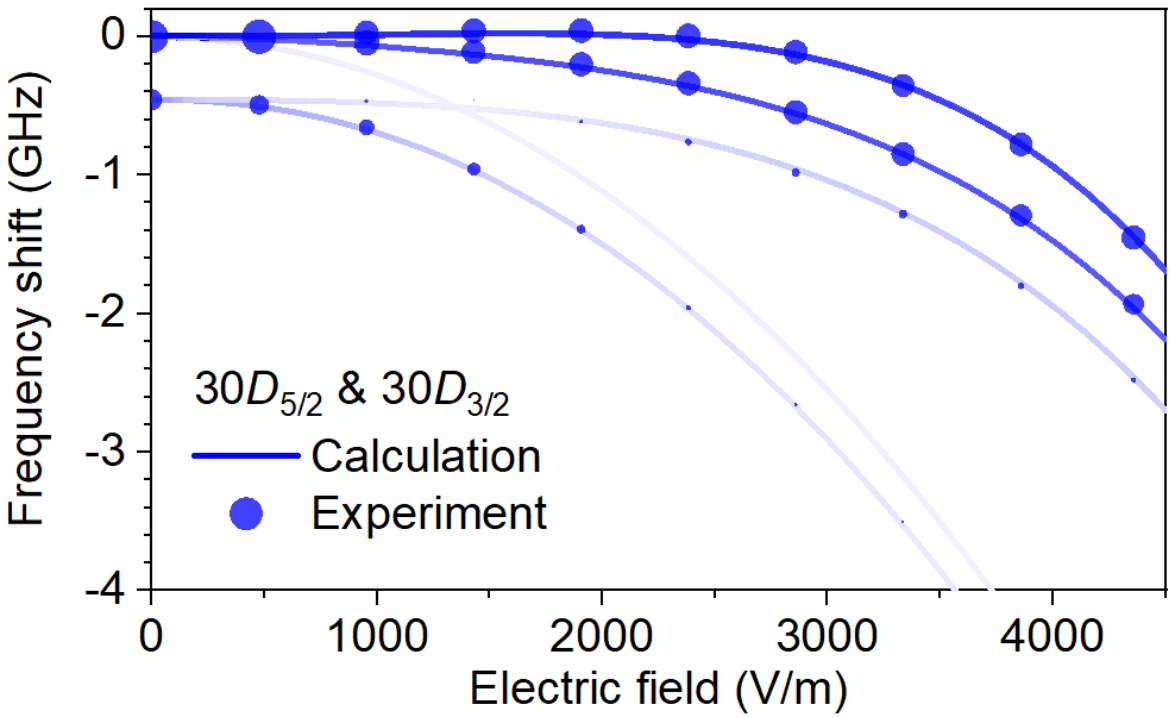

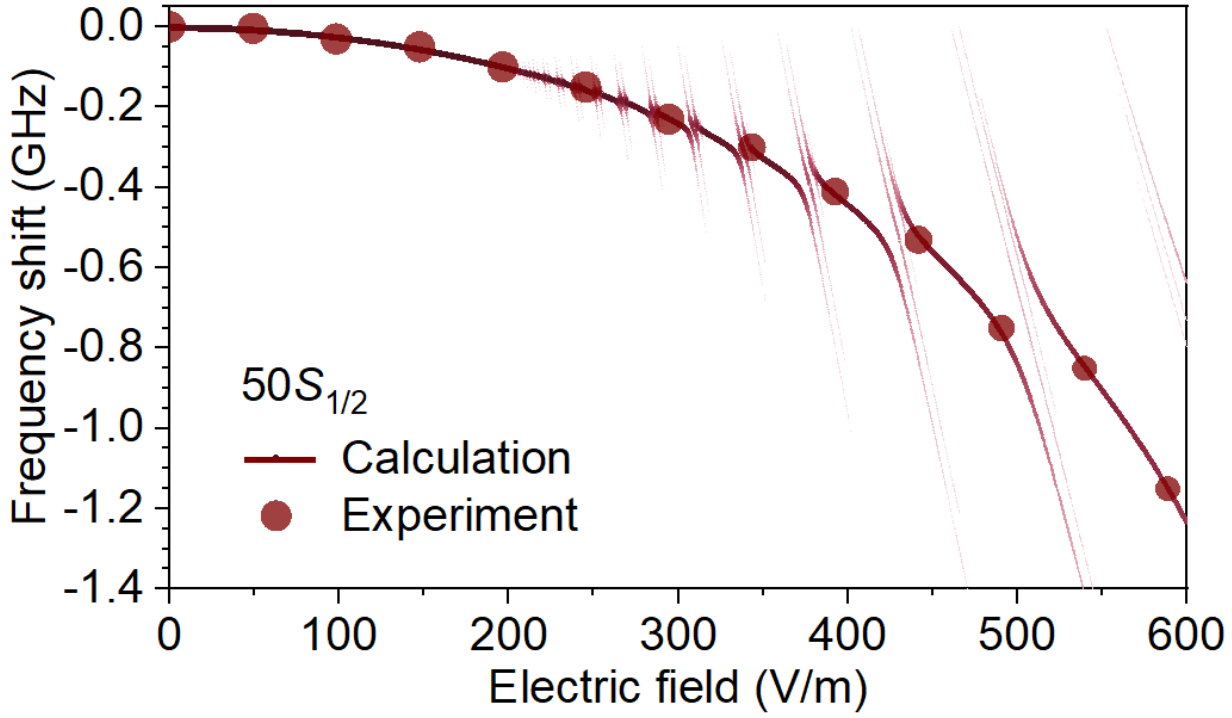

Density-matrix modeling of EIT and the method of producing the detected E-field signals

Atomic density-matrix modeling

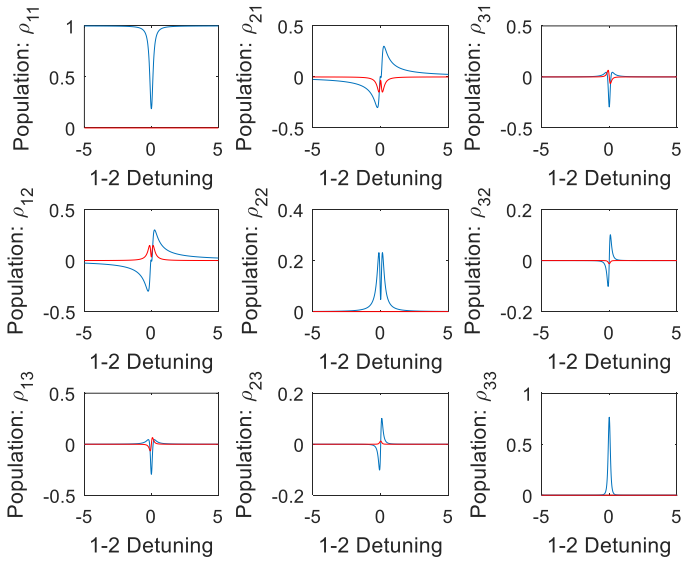

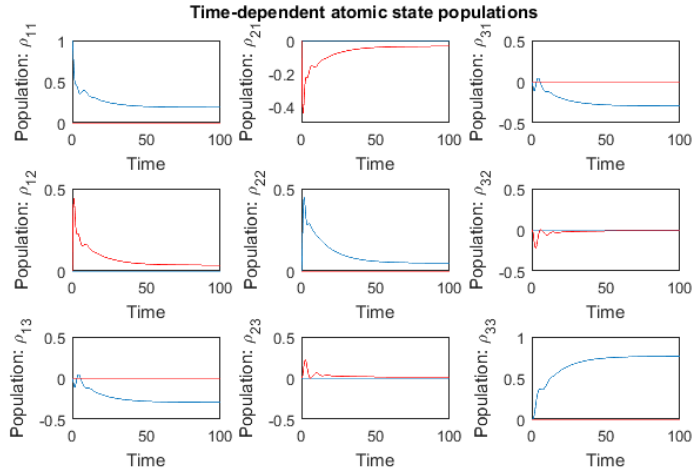

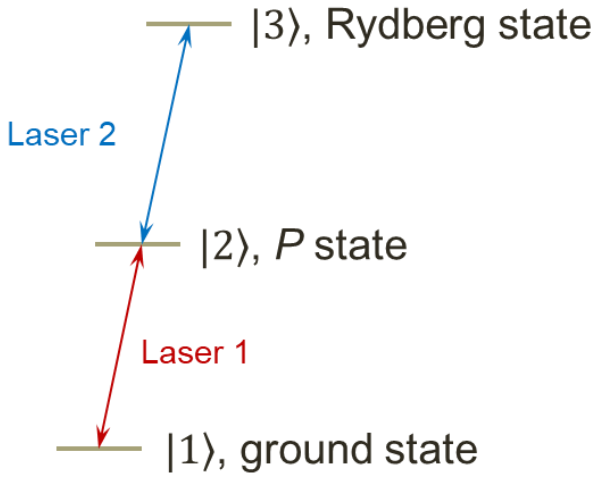

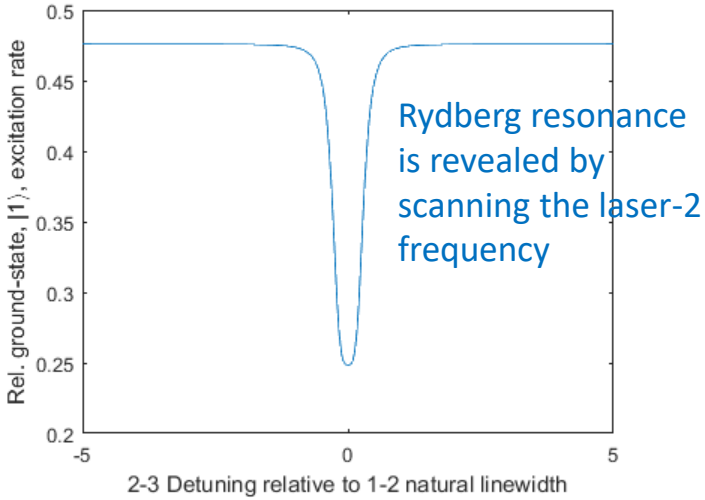

Convert a resonance signal to an error signal by dithering the laser-2 frequency

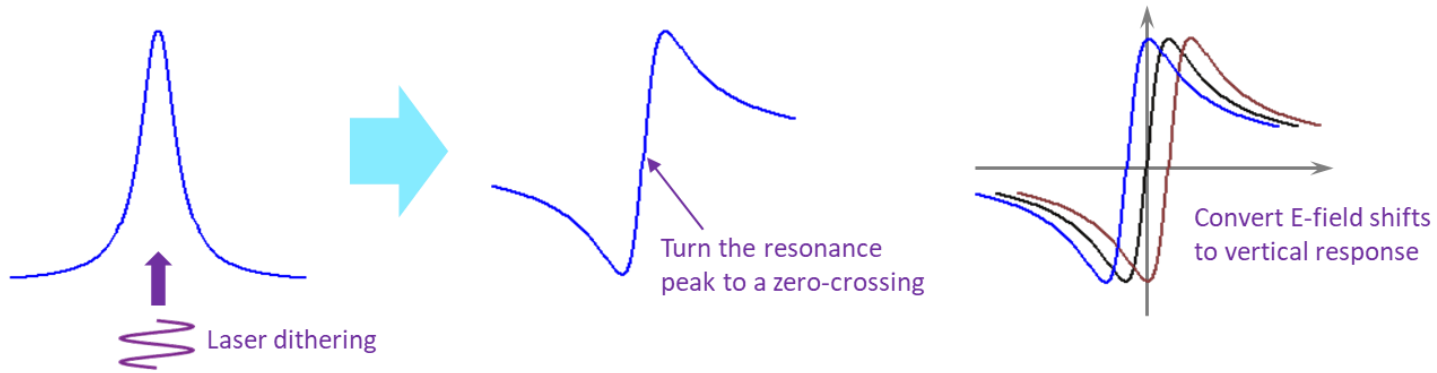

Problem of E-field screening effect of the alkali-vapor cell

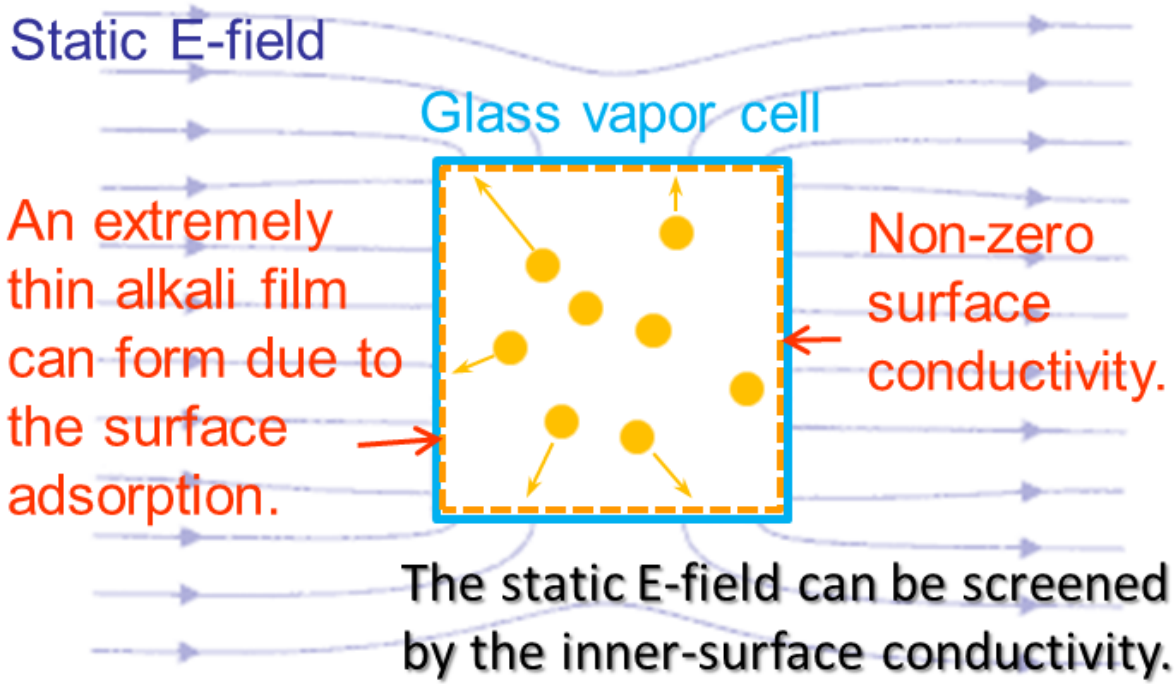

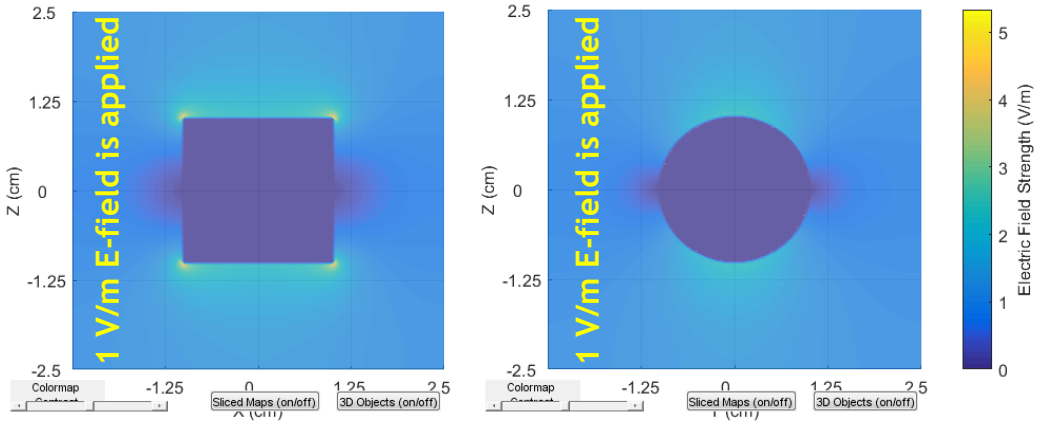

The major technical challenge of using alkali vapor inside a glass cell is the screening effect to the external static or low-frequency E-fields due to surface adsorption of alkali-metal atoms. The low-frequency sensitivity is limited by the inner-surface conductivity of the vapor cell. Normally, the SiO_2 based alkali-vapor cells have $R_s \sim 100\ \mathrm{k\Omega}$ with alkali vapor.

To have a more-quantitative understanding, we can consider an analytically solvable case: a spherical vapor cell with radius r and negligible glass thickness, and we find $E_i(t) = E_e \exp(-t/1.5\epsilon R_s r)$, where $E_i(t)$ is the time dependent, internal-electric-field amplitude caused by the externally applied, uniform electric field, which suddenly turns on at t = 0 and has amplitude E_e, is the effective electric permittivity of the space, and R_s is the sheet resistance on the inner surface. Thus, the E-field screening becomes significant when the frequency of the electric field is lower than $1/(2\pi \times 1.5\epsilon R_s r)$.

Improving vapor-cell E-field screening problem – Sapphire cell

The common materials for making alkali-vapor cells are fused-silica glass, borosilicate glass, aluminosilicate glass, and other silicon-oxide based glass. The earlier research work has shown that sapphire material can be very resistant to alkali-metal atoms and have lower surface adsorption compared to SiO_2 based glass.

Sapphire alkali vapor cell made by Japan Cell Inc.

- The US does not have vendors making sapphire vapor cells. We ordered sapphire Rb vapor cells from Japan Cell Inc.
- Sandia may also have the capability to brace sapphire materials together to assemble a sapphire vapor cell.
- Sandia also has the capability of doing ALD of Al_2O_3 on the inner surface of SiO_2 based glass cells. This may provide inner surface conditions similar to a pure sapphire cell.
- Alkali vapor cells made of sapphire should have lower electrical conductivity on the inner surface.

Experiments of E-field screening on a sapphire-made Rb cell

All sapphire made Rb-vapor cell is relatively difficult to manufacture and therefore hard to implement electrodes with it. No direct resistance measurement can be achieved. We can, however, directly measure the E-field screening time constant by looking at the 50S Rydberg signal responding to the external E-field.

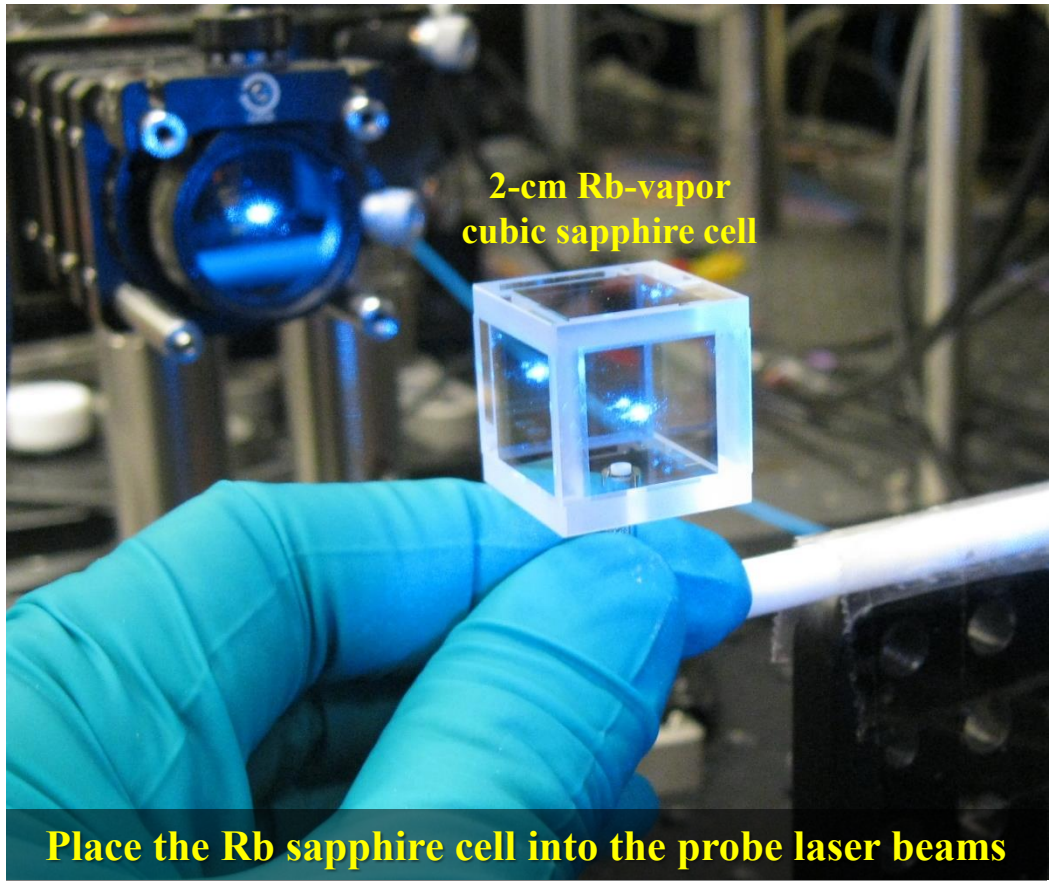

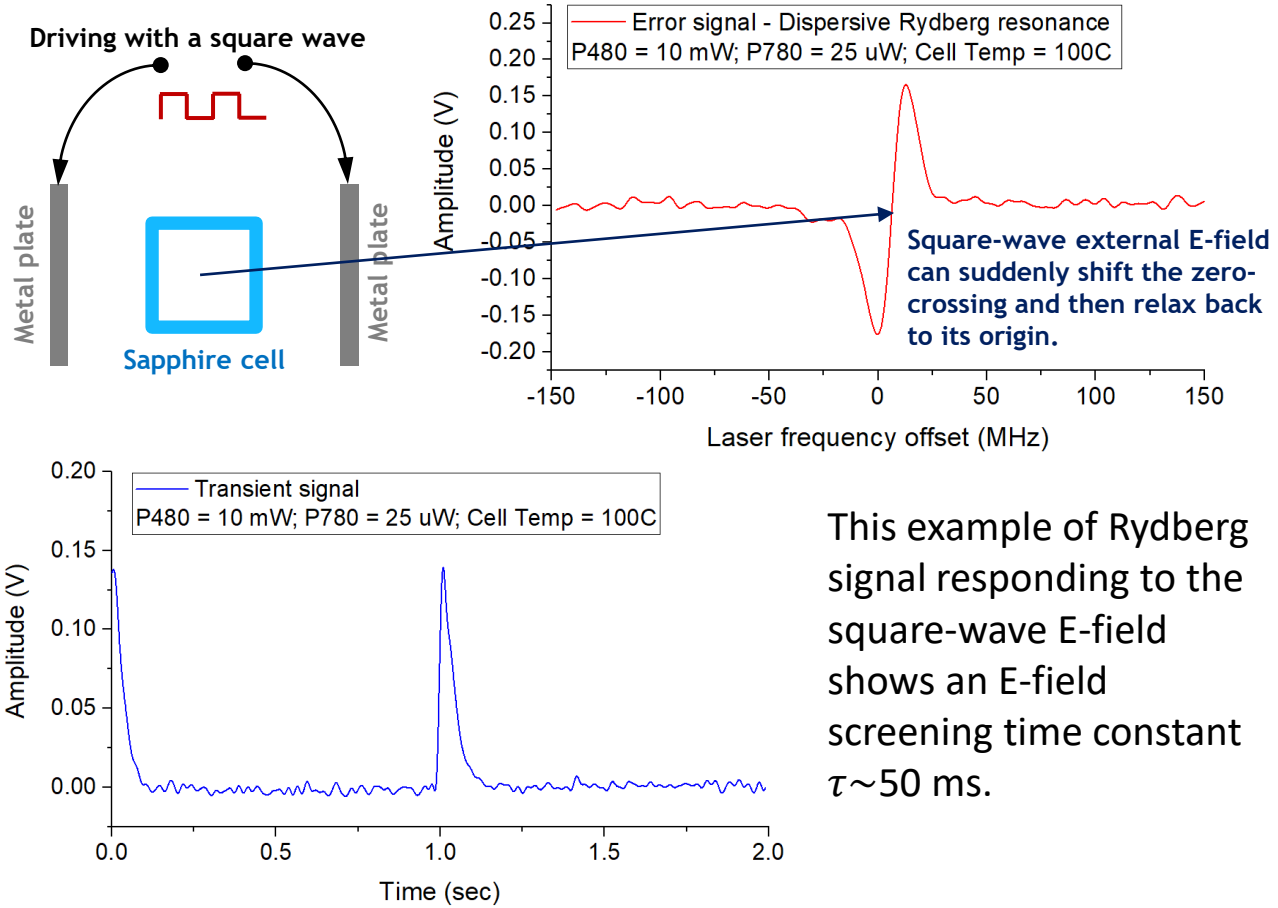

This example of Rydberg signal responding to the square-wave E-field shows an E-field screening time constant $\tau \sim 50$ ms.

Sheet Resistance on the inner surface of a Rb sapphire cell

The inner surface square resistance R_s can be determined from the E-field screening rate ($= 1/\tau$) measurements. We find the intrinsic (zero laser power) R_s **on the order of 10^{12} Ω!**

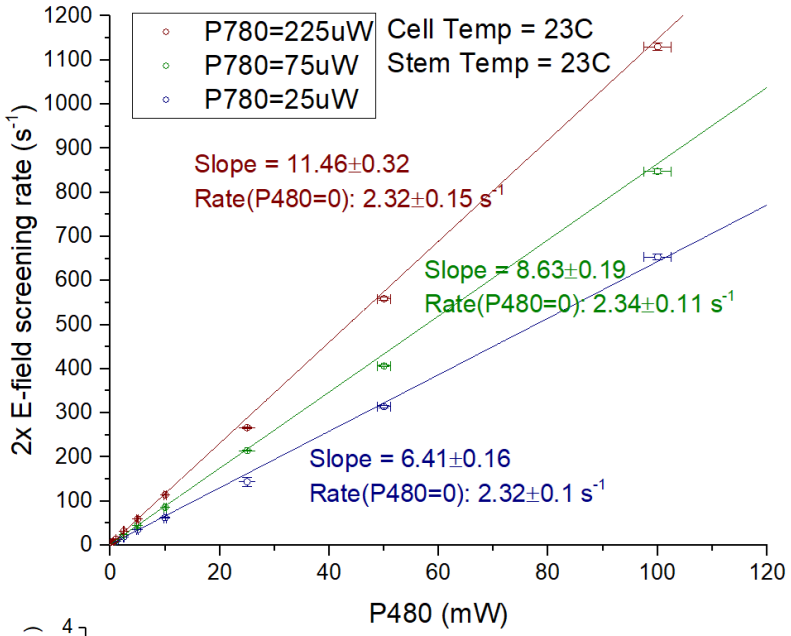

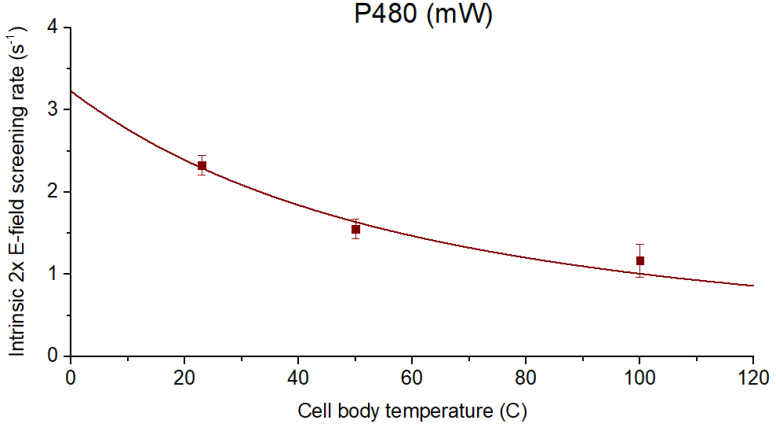

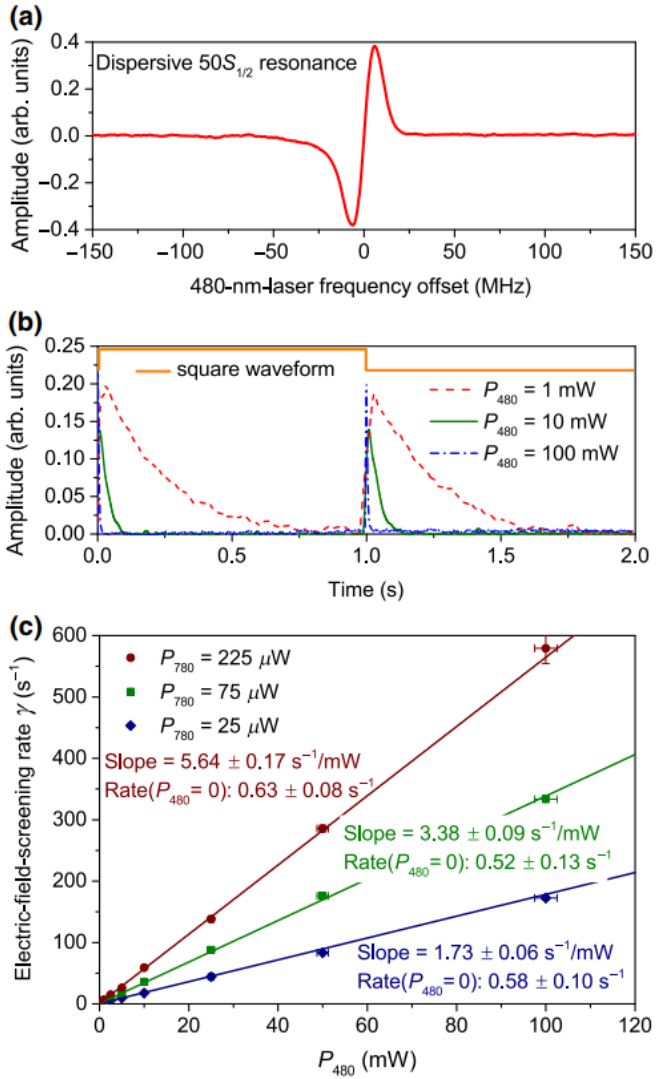

External E-field detection with sapphire cell

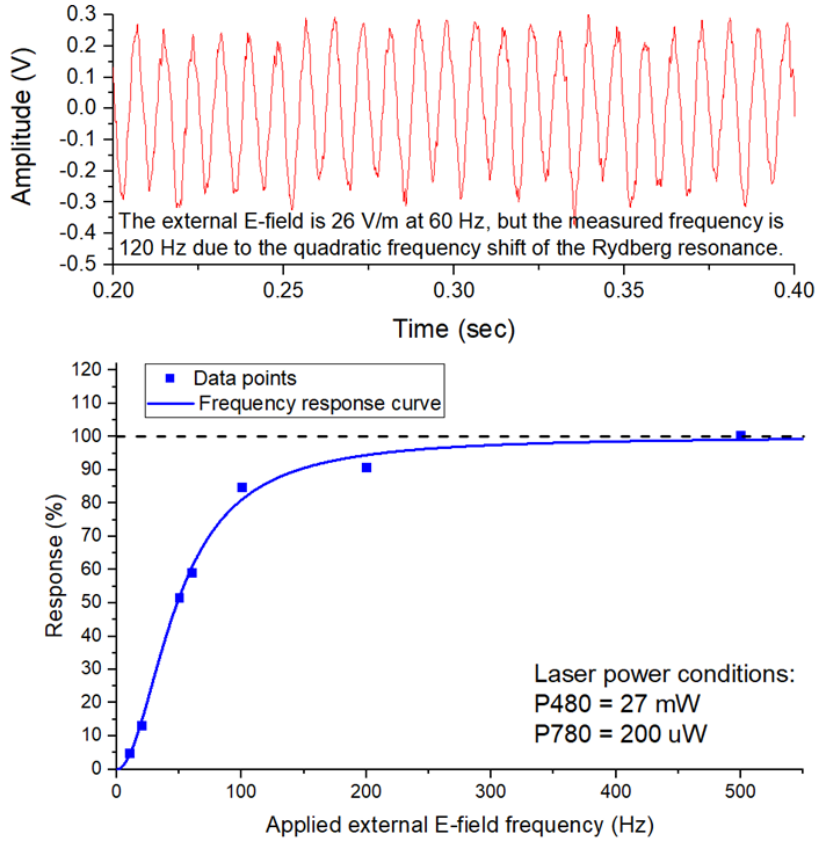

We find the R_s without the presence of the 480-nm laser to be **2.3, 3.4, and 4.7 TΩ** for cell temp. = 23, 50, and 100°C.

Performing ultra-low-frequency atomic electrometry

We use LED light to induce bias E-field inside the vapor cell. The Rydberg state for E-field sensing is $100S_{1/2}$. By increasing the LED current, more bias E-field can be generate to improve the signal size until the inhomogeneous effect of the LED induced bias field takes over the linewidth broadening.

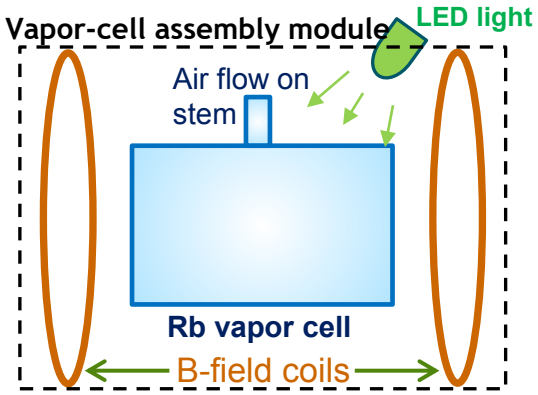

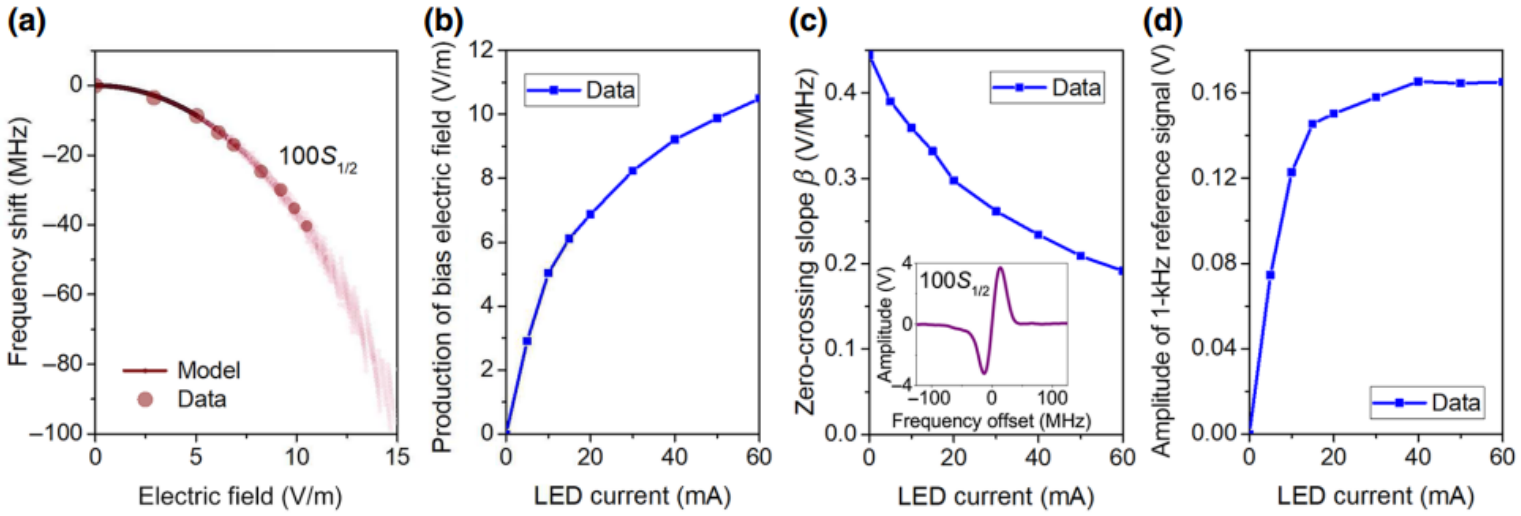

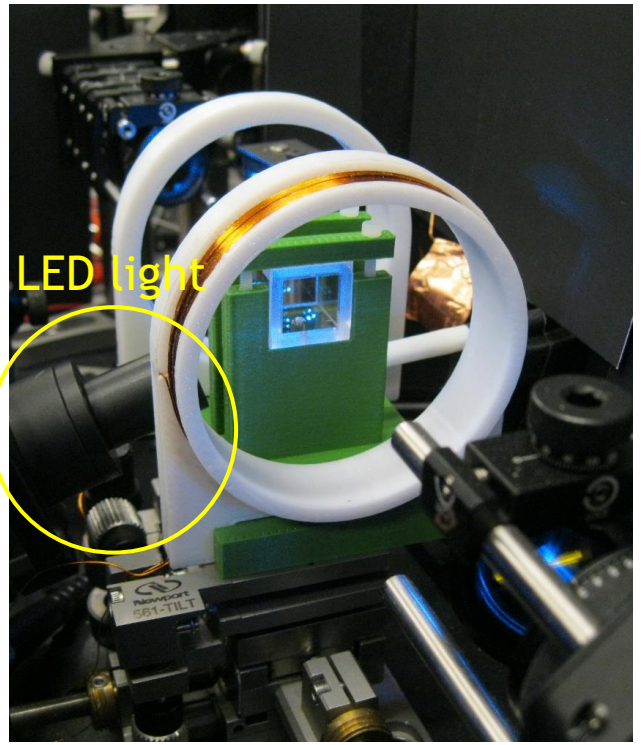

FIG. 6. (a) Modeling and experimental results for the electric-field-dependent $100S_{1/2}$-resonance shift. (b) Amplitude of the optically induced bias electric field inside the sapphire cell versus I_{LED}. (c) The slope at the zero crossing of the dispersive $100S_{1/2}$ resonance versus I_{LED}. The inset shows the corresponding dispersive resonance at zero bias electric field. (d)The measured signal amplitude of the electric field reference signal at 1 kHz versus I_{LED}.

Pictures of atomic E-field sensing of charged objects

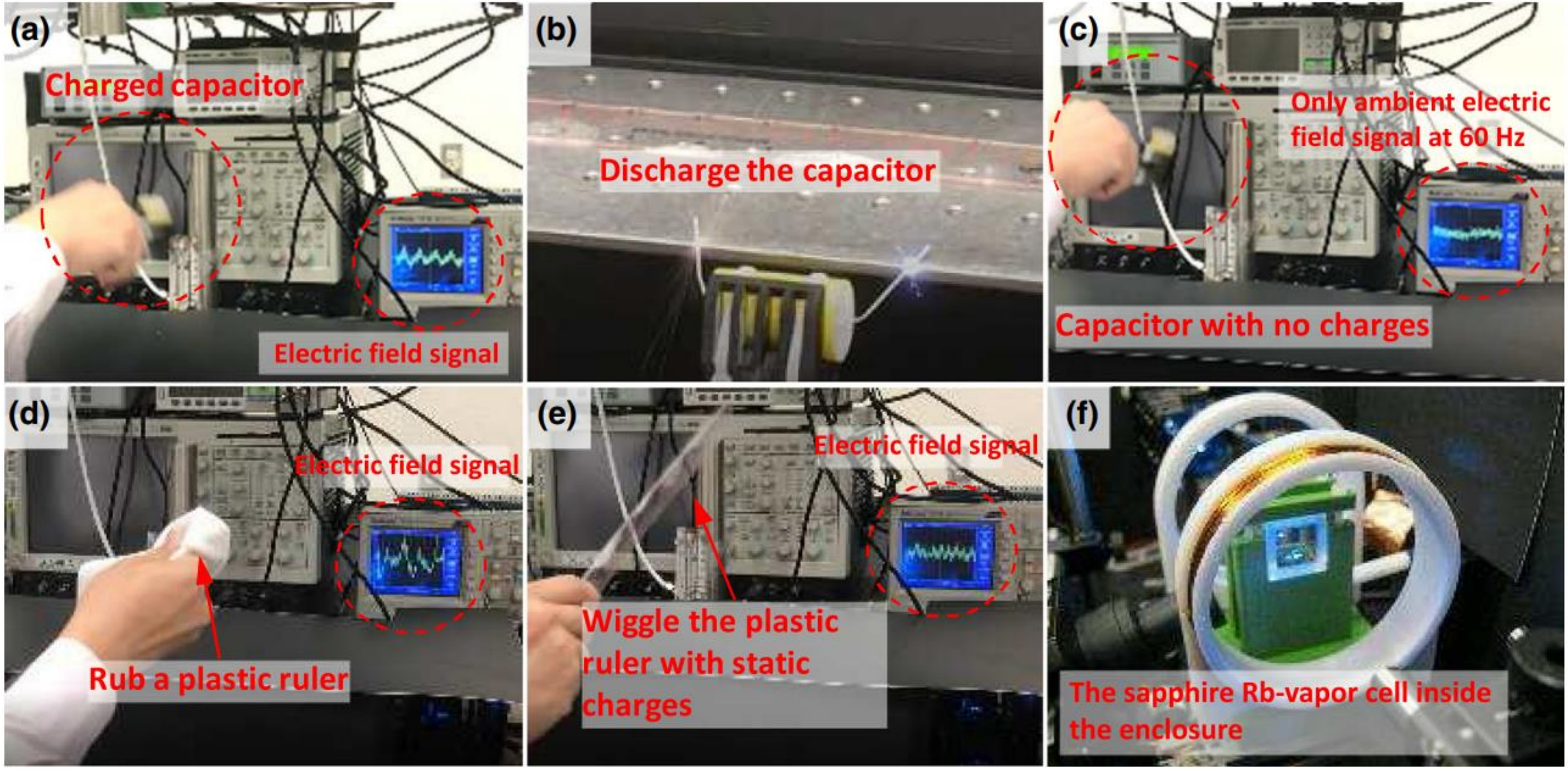

Video demo

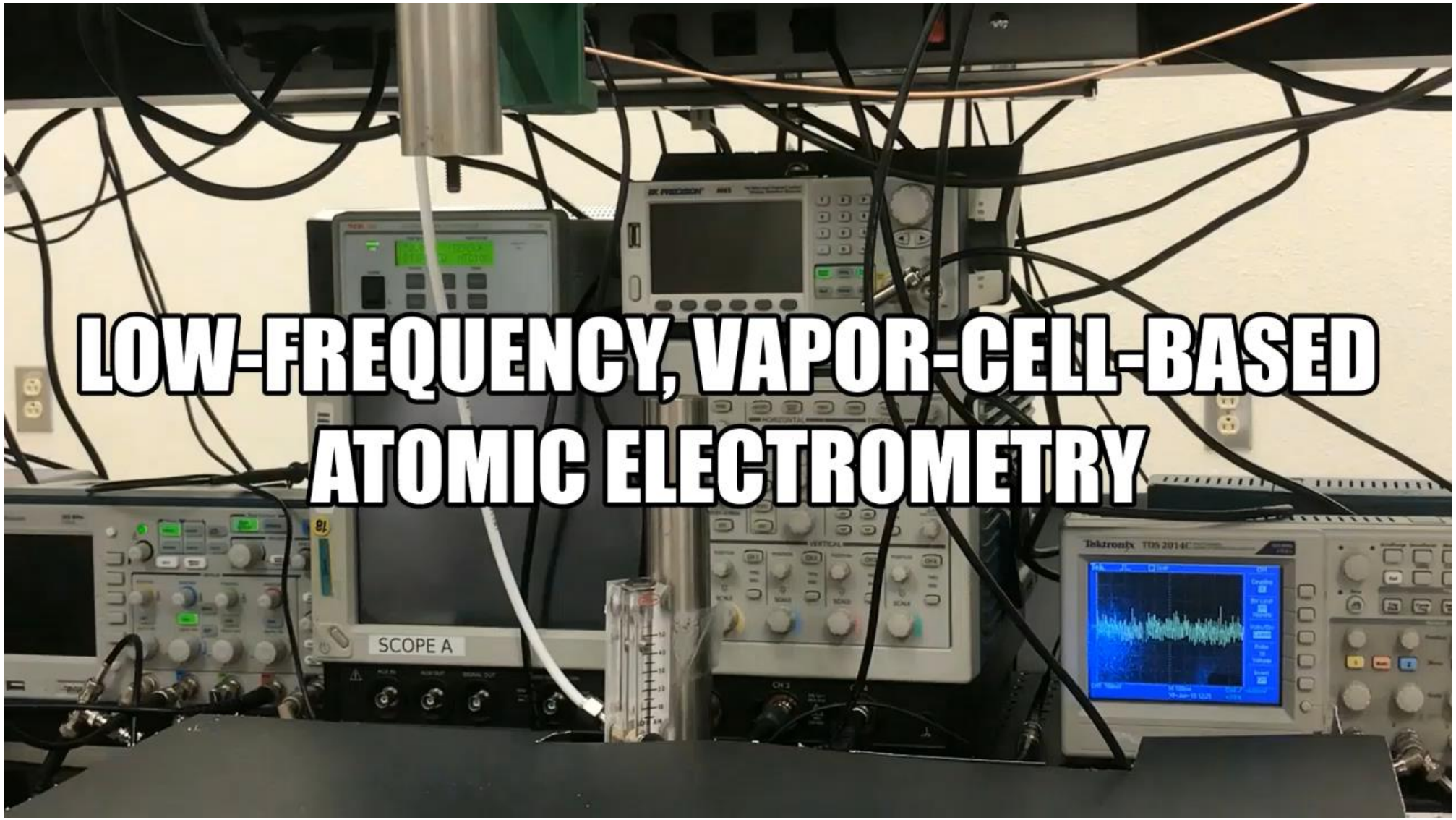
LOW-FREQUENCY, VAPOR-CELL-BASED
ATOMIC ELECTROMETRY
SCOPE A
Tektronix

Spectral noise floor of Sandia's ULF atomic electrometer

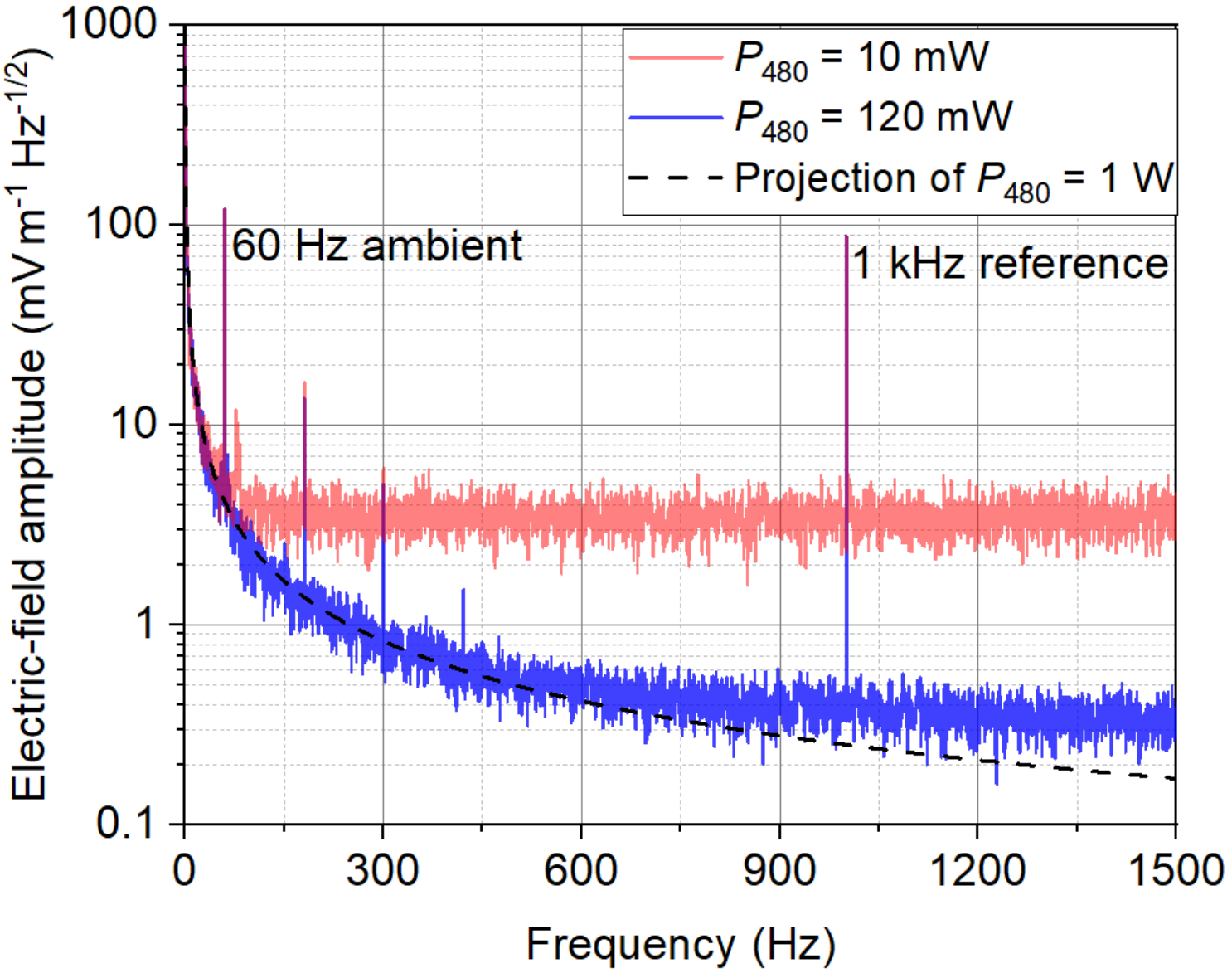

We demonstrated in-vapor E-field sensitivity about 340 μV/m per $Hz^{1/2}$ for frequency from DC to 10 kHz.

Due to the E-field screening effect on the vapor cell, the actual sensitivity for external E-field has to be corrected as shown on the left plot.

Comparison of the ULF electric-field sensor technologies

Technology	Best Demonstrated Sensitivity	Direct E-field Measurement	Absolute Measurement	Sensing Volume	Dynamic Range	Major Advantages	Disadvantages
Alkali-metal Rydberg atom	340 μV/(m·Hz$^{1/2}$) @ quasi-DC to VLF Sandia's demonstration	Yes	Yes	mm^3 ~ cm^3	60 dB ~ 120 dB	• Direct E-field measurement • Absolute measurement • Small sensing volume	• Require lasers • E-field screening issue of the alkali atom container
Electro-optic (EO) Effect	5 mV/(m·Hz$^{1/2}$) @ SLF to EHF	Yes	No	~ sub-cm^3	~ 130 dB	• Very broadband • Very large dynamic	• Temp. sensitivity • Bias drifts
Single NV center in diamond	90 kV/(m·Hz$^{1/2}$) @ DC 10 V/(m·Hz$^{1/2}$) @ ULF, multiple NVs, sensing volume = 10^6 μm^3	Yes	No	~ nm^3	NA	• Very high spatial resolution	• Poor sensitivity • High laser power
Single quantum dot	5 V/(m·Hz$^{1/2}$) @ quasi-DC to ULF	No	No	~ sub-μm^3	NA	• High spatial resolution	• 4.2 K environment • Bias drifts
MEMs	100 V/(m·Hz$^{1/2}$) @ quasi-DC to SLF	Yes or No	No	~ mm^3	~ 50 dB	• Fabrication technology • Simple mechanism	• Temp. sensitivity • Bias drifts
Differential Electric potential probes	1 μV/(m·Hz$^{1/2}$) @ quasi-DC to HF	No	No	~ m^3	40 dB ~ 80 dB	• All electronic	• Very large sensing volume • Bias drifts
E-field Mill	3 mV/(m·Hz$^{1/2}$) @ quasi-DC to ELF	No	No	~ 1000 cm^3	~ 120 dB	• Large dynamic range	• Large sensing vol. • Bias drifts

DC	ELF	SLF	ULF	VLF	LF	MF	HF	VHF	UHF	SHF	EHF
0Hz	3-30Hz	30-300Hz	300Hz-3kHz	3-30kHz	30-300kHz	300kHz-3MHz	3-30MHz	30-300MHz	300MHz-3GHz	3-30GHz	30-300GHz

Outlook – Applications of ULF atomic E-field sensor

We have made significant progress in ultra-low-frequency atomic E-field sensor. We expect a broad application space of this new technology once it is fully developed.

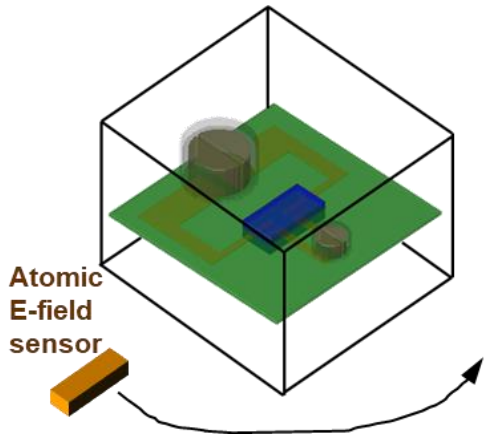

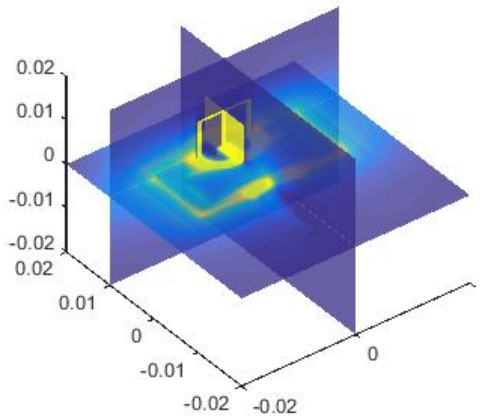

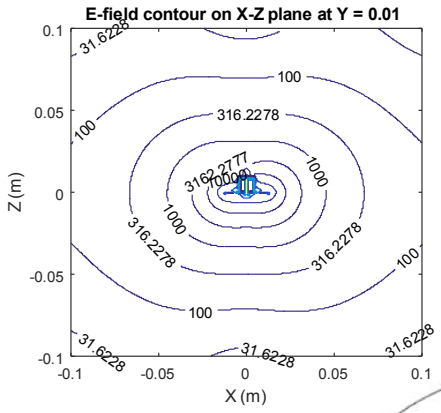

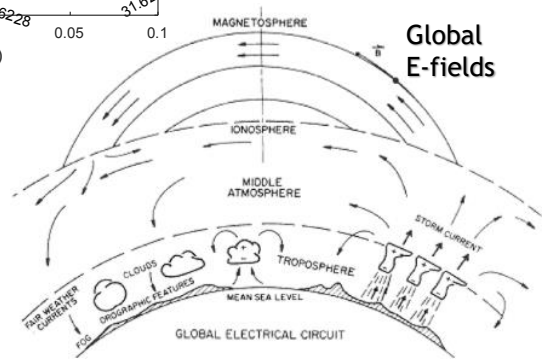

- Noninvasive diagnostics of electronics in extremely-low-current mode that has only voltage signatures
- Electric-field signal source localization & E-field gradiometry
- Proximity detection and remote activities surveillance
- Wireless communication at ELF and SLF bands
- Geoscience study via E-field measurements
- Bioscience study through E-field signals